# The stability of sodalite in the system NaAlSiO$_4$-NaCl*

Z. D. SHARP[1,†], G. R. HELFFRICH[2], S. R. BOHLEN[3,‡] and E. J. ESSENE[4]

[1] Geophysical Laboratory, Carnegie Institution of Washington, 2801 Upton Street, N.W., Washington, D.C. 20008, U.S.A.
[2] Department of Geological Sciences, Northwestern University, Evanston, IL 60208, U.S.A.
[3] Department of Earth and Space Sciences, S.U.N.Y, Stony Brook, NY 11794, U.S.A.
[4] Department of Geological Sciences, University of Michigan, Ann Arbor, MI 48109, U.S.A.

**Abstract**—The reaction sodalite = $\beta$-nepheline + NaCl ($s$) was reversed in solid-medium apparatus (923 K, 7.6–8.0 kbar; 973 K, 7.4–7.6 kbar; 1073 K, 7.8–8.0 kbar; 1173 K, 8.4–8.6 kbar) and the reaction sodalite = carnegieite + NaCl ($l$) was reversed at 1 bar (1649–1652 K). The calculated slope for the first reaction is $-11$ bar/K compared to the experimentally constrained slope above 973 K of $+5$ bar/K. This major discrepancy can be eliminated if the entropy of sodalite (Na$_8$Al$_6$Si$_6$O$_{24}$Cl$_2$) is 61.7 J/mol · K greater than the measured value of 848.1 ± 4.0 J/mol · K at 298.15 K. This entropy contribution is equal to that expected from 58% disorder of Al and Si on the tetrahedral sites, but could also be caused by a reversible phase change. The experimental reversals between 923 K and 973 K can be fit with a $dP/dT$ of $-11$ bar/K, suggesting that the excess entropy for sodalite is present only above 923 K. A phase diagram for the NaAlSiO$_4$-NaCl system that is consistent with the measured thermochemical data and the experiments between 973 and 1650 K can be generated if the 61.7 J/mol · K entropy contribution is included in the $S^0_{298}$ of sodalite. This entropy contribution must be removed below 973 K for the experiments to fit with calculations. Previously unreported thermodynamic data estimated in this study are $\Delta G^0_{298}$ for sodalite ($-12697$ kJ/mol) and carnegieite (NaAlSiO$_4$) ($-1958$ kJ/mol), $S^0_{298}$ of carnegieite (129.6 J/mol·K) and compressibility of NaCl$_{liquid}$ ($V^F_{298}$ (cm$^3$) = 31.6·[1 − 24.7·10$^{-3}$·$P$ + 800·10$^{-6}$·$P^2$]) ($T$ in K; $P$ in kbar).

Sodalite is a high-temperature, low-pressure phase, stable well above the solidus in sodic silica-undersaturated magmas enriched in NaCl, and its presence constrains NaCl activities in magmas. Estimates of minimum NaCl ($l$) activities in the Mont St-Hilaire sodalite syenites are 0.05 at 1073 K and 0.13 at 1273 K. Density calculations are consistent with the field observations that sodalite phenocrysts will float in a nepheline syenite liquid. This explains the enrichment of sodalite in the upper levels of the sodalite syenites at Mont St-Hilaire and elsewhere.

## INTRODUCTION

THE PRESENCE AND composition of fluids in high-temperature, geological environments have a strong effect on the physical and chemical properties of solids and melts and will in large part determine the final mineral assemblage of rocks exposed at the Earth's surface. Measurement of fluid inclusion salinities has been used widely as an indication of fluid salinity at the time of crystallization of the host mineral (*e.g.*, ROEDDER, 1984); however, these fluids are often trapped or last-modified well after crystallization and need not constrain conditions extant at the time of the crystallization of the host. Phase equilibria have only rarely been used to calculate fluid salinities because of a lack of mineral assemblages that buffer the activity of NaCl. One of the few rock-forming minerals that contains chlorine as an essential component is sodalite (Na$_8$Al$_6$Si$_6$O$_{24}$Cl$_2$). It is restricted to rocks undersaturated in SiO$_2$ and found most commonly in hdyrothermally altered

igneous rocks (DEER *et al.*, 1963; CARMICHAEL *et al.*, 1974), although it is occasionally reported as a primary phase in alkali layered intrusions (*e.g.*, USSING, 1912; VLASOV *et al.*, 1966), in metamorphic rocks (SIMPSON and OTTO, 1960) and in meteorites (GROSSMAN and STEELE, 1976; LUMPKIN, 1980). With accurate thermodynamic data for phases in the NaAlSiO$_4$-NaCl system, the activity of NaCl may be calculated in sodalite and nepheline-bearing rocks and constrained in undersaturated rocks that do not contain sodalite. Available thermodynamic data were combined with experimental equilibrium reversals for the reaction

$$6 \text{ NaAlSiO}_4 + 2 \text{ NaCl} = \text{Na}_8\text{Al}_6\text{Si}_6\text{O}_{24}\text{Cl}_2 \qquad (1)$$
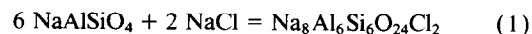
in order to calculate the stability field of sodalite-bearing assemblages.

Comprehensive studies of sodalite stability relations were made by Wellman, who determined the decomposition temperatures of sodalite at low NaCl fugacities (WELLMAN, 1969a,b) and in dilute aqueous solutions (WELLMAN, 1970a). WELLMAN (1970b) also derived activity coefficients for NaCl in aqueous solution at elevated temperatures and pressures from his experiments. STORMER and CARMICHAEL (1971) used the decomposition data of WELLMAN (1969b) to derive free energy data for sodalite at elevated temperatures. BARKER (1976) evaluated the relations between sodalite and analcime as a function of temperature and salinity, and BINSTED

---

(1981b) determined the breakdown temperature of sodalite at various pressures, as well as the liquidus relations in the system $NaAlSiO_4$-$SiO_2$-NaCl-$H_2O$ at 1 kbar (BINSTED, 1981a). In this study the first reversed experiments of reaction (1) at elevated pressure are reported and a thermodynamically consistent set of data are derived for the phases in the system $NaAlSiO_4$-NaCl.

## NOMENCLATURE AND SUMMARY OF PHASES IN THE SYSTEM NaAlSiO₄-NaCl

Sodalite is the only known polymorph of $Na_8Al_6Si_6O_{24}Cl_2$, although HAZEN and SHARP (1988) observed crystal deterioration above 30 kbar (298 K) which may be due to a reconstructive transition to a high-pressure form. Halite (NaCl($s$)), liquid NaCl (NaCl($l$)) and NaCl($v$) are the phases of NaCl considered in this study. There are at least six known phases of $NaAlSiO_4$. These include several high-pressure phases, three nepheline polymorphs and two carnegieite polymorphs. KELLEY et al. (1953) defined the nepheline polymorphs as $\delta$-nephelite (298–467 K), $\beta$-nephelite (467–1180 K) and $\gamma$-nephelite (1180–1525 K). ROBIE et al. (1978) defined the 467 K transition as the $\alpha$-$\beta$ transition. In this paper, the three phases (with increasing temperature) are $\alpha$-$\beta$- and $\gamma$-nepheline. The two carnegieite polymorphs have been defined by KELLEY et al. (1953) as the $\delta$-carnegieite (298–980 K) and $\beta$-carnegieite (980–1700 K). For consistency, the low- and high-temperature polymorphs of carnegieite are defined as $\alpha$-carnegieite and $\beta$-carnegieite, respectively.

## EXPERIMENTAL PROCEDURE

### Starting materials

The sodalite used for all experiments was collected from a sodalite-syenite body exposed in the DeMix quarry, Mont St-Hilaire, Quebec (CURRIE et al., 1986). Its composition was determined with an automated Cameca CAMEBAX microprobe at the University of Michigan (Table 1). Because feldspathoids are especially prone to beam damage (e.g., BROUSSE et al., 1969; AUTEFAGE, 1980), operating conditions were carefully chosen to minimize volatilization. The degree of volatilization of sodium in halite, sodalite and nepheline was

Table 1. Chemical analyses of selected sodalite and nepheline samples. Sodalite normalized to 12 tetrahedral cations, nepheline normalized to 2 tetrahedral cations. Analytical method: Ilímaussaq (Ussing, 1912); Lovozero (Vlasov et al., 1966); wet chemical. All others (this study); electron microprobe. (MSH - Mont St-Hilaire, ISQ - Ilimaussaq, PC - piston cylinder, sod - sodalite, ne - nepheline, n.d. - not determined)

|  | sod MSH | sod PC-15 | sod ISQ | sod LOV | ne PC-7 | ne PC-17 |
|---|---|---|---|---|---|---|
| $SiO_2$ | 37.09 | 37.62 | 36.50 | 36.99 | 43.27 | 43.39 |
| $Al_2O_3$ | 31.53 | 32.99 | 31.53 | 31.77 | 35.99 | 36.22 |
| $Fe_2O_3$ | 0.32 | n.d. | 0.19 | 0.17 | n.d. | n.d. |
| CaO | n.d. | n.d. | n.d. | 0.05 | n.d. | n.d |
| $Na_2O$ | 24.73 | 25.03 | 26.30 | 25.84 | 21.45 | 21.50 |
| $K_2O$ | 0.10 | 0.00 | 0.18 | 0.16 | 0.00 | 0.00 |
| $Cl_2$ | 6.87 | 7.02 | 7.30 | 6.44 | 0.06 | 0.26 |
| $S_2$ | 0.08 | n.d. | n.d. | 0.39 | n.d. | n.d. |
| -O=Cl,S | 1.59 | 1.59 | 1.65 | 1.65 | 0.01 | 0.06 |
| Total | 99.06 | 101.07 | 100.60 | 100.16 | 100.75 | 101.26 |
| Si | 5.98 | 5.90 | 5.93 | 5.95 | 1.01 | 1.01 |
| Al | 5.99 | 6.10 | 6.04 | 6.03 | 0.99 | 0.99 |
| $Fe^{3+}$ | 0.04 | n.d. | 0.02 | 0.02 | n.d. | n.d. |
| Ca | n.d. | n.d. | n.d. | 0.01 | n.d. | n.d. |
| Na | 7.72 | 7.61 | 8.30 | 8.06 | 0.97 | 0.97 |
| K | 0.02 | 0.00 | 0.04 | 0.03 | 0.00 | 0.00 |
| Cl | 1.88 | 1.87 | 2.02 | 1.76 | 0.00 | 0.01 |
| S | 0.02 | n.d. | n.d. | 0.12 | n.d. | n.d. |
| O | 23.90 | 23.82 | 24.15 | 24.02 | 3.99 | 3.99 |

Table 2. X-ray data for Mont St-Hilaire (MSH) sodalite and synthetic sodalite and nepheline from this study.

sodalite, MSH
a = 8.8791(7)

| hkl | d(obs) | d(calc) | I |
|---|---|---|---|
| 110 | 6.28 | 6.28 | 100 |
| 200 | 4.45 | 4.44 | 7 |
| 210 | 3.98 | 3.97 | 1 |
| 211 | 3.63 | 3.62 | 19 |
| 222 | 2.564 | 2.563 | 4 |
| 321 | 2.373 | 2.373 | 7 |
| 400 | 2.218 | 2.220 | 1 |
| 330 | 2.094 | 2.093 | 6 |
| 420 | 1.986 | 1.985 | 1 |
| 422 | 1.813 | 1.812 | 1 |
| 510 | 1.742 | 1.741 | 2 |
| 521 | 1.621 | 1.621 | 1 |
| 440 | 1.570 | 1.570 | 5 |
| 600 | 1.480 | 1.480 | 8 |
| 611 | 1.440 | 1.440 | 2 |
| 541 | 1.370 | 1.370 | 1 |
| 622 | 1.339 | 1.339 | 1 |
| 721 | 1.208 | 1.208 | 1 |

sodalite (1644 K, 1 bar)
a = 8.8839(9)

| hkl | d(obs) | d(calc) | I |
|---|---|---|---|
| 110 | 6.30 | 6.28 | 69 |
| 200 | 4.45 | 4.44 | 9 |
| 211 | 3.63 | 3.63 | 100 |
| 222 | 2.564 | 2.565 | 15 |
| 321 | 2.375 | 2.374 | 19 |
| 330 | 2.094 | 2.094 | 20 |
| 422 | 1.813 | 1.813 | 2 |
| 440 | 1.570 | 1.570 | 7 |
| 600 | 1.480 | 1.481 | 3 |
| 611 | 1.442 | 1.441 | 2 |
| 541 | 1.371 | 1.371 | 5 |
| 622 | 1.339 | 1.334 | 3 |
| 721 | 1.209 | 1.209 | 2 |

sodalite (1173 K, 8.4 kbar)
a = 8.879(2)

| hkl | d(obs) | d(calc) | I |
|---|---|---|---|
| 110 | 6.29 | 6.28 | 73 |
| 211 | 3.63 | 3.63 | 100 |
| 222 | 2.565 | 2.563 | 15 |
| 321 | 2.374 | 2.373 | 14 |
| 330 | 2.092 | 2.093 | 16 |
| 600 | 1.480 | 1.480 | 5 |

nepheline (1273 K, 10 kbar)
a = 9.972(1), c = 8.333(1)

| hkl | d(obs) | d(calc) | I |
|---|---|---|---|
| 002 | 4.17 | 4.17 | 90 |
| 201 | 3.83 | 3.83 | 100 |
| 211 | 3.039 | 3.039 | 5 |
| 202 | 2.998 | 2.998 | 95 |
| 300 | 2.878 | 2.879 | 15 |
| 212 | 2.569 | 2.570 | 10 |
| 220 | 2.493 | 2.493 | 5 |
| 203 | 2.336 | 2.336 | 20 |
| 213 | 2.116 | 2.115 | 10 |

nepheline (1373 K, 1 bar)
a = 9.985(2), c = 8.322(2)

| hkl | d(obs) | d(calc) | I |
|---|---|---|---|
| 002 | 4.16 | 4.16 | 75 |
| 201 | 3.83 | 3.84 | 100 |
| 202 | 2.998 | 2.998 | 100 |
| 300 | 2.882 | 2.882 | 15 |
| 203 | 2.335 | 2.335 | 20 |
| 311 | 2.305 | 2.305 | 10 |
| 310 | 2.399 | 2.398 | 10 |

nepheline (1073 K, 8 kbar)
a = 9.978(2), c = 8.332(2)

| hkl | d(obs) | d(calc) | I |
|---|---|---|---|
| 002 | 4.17 | 4.17 | 65 |
| 201 | 3.84 | 3.84 | 95 |
| 211 | 3.042 | 3.041 | 5 |
| 202 | 2.999 | 2.999 | 100 |
| 300 | 2.880 | 2.880 | 30 |
| 203 | 2.336 | 2.336 | 35 |
| 213 | 2.115 | 2.116 | 10 |

evaluated at various operating conditions. Short (2 sec) successive counting periods were made on a single rastered area for an extended time period. For the operating conditions of 5 kV accelerating voltage, 5 nA beam current, with a beam rastered over 3 $\mu m^2$, there was no detectable sodium loss. These operating conditions were used to analyze for Na, Al, Si, S and Cl; operating conditions were increased to 12 kV and 12 nA for analysis of K and Fe. The sodium content of sodalite is greater than that of any other aluminosilicate, so halite was used as a standard for both sodium and chlorine. The other standards employed were andalusite for Al, albite for Si, potassium feldspar for K, acmite for Fe and anhydrite for S. Because of the low accelerating voltage and the dominance of light elements, it was critical to carbon-coat samples and standards simultaneously. The composition of sodalite determined in this study is in agreement with a previous analysis (PETERSON, 1983) of sodalite from the same locality. Nevertheless, the calculated site vacancies (Table 1) have a high uncertainty due to the susceptibility of sodalite to beam damage. Previous sodalite analyses with the electron microprobe also require a large vacancy contribution, presumably as a result of volatilization of sodium and chlorine (e.g., AUTEFAGE, 1980). In contrast, wet chemical analyses of sodalite (USSING, 1912; VLASOV et al., 1966; Table 1) do not require any vacancy contributions. For the purposes of phase equilibrium calculations, site vacancies were considered to be artifacts of the analytical technique and were ignored.

The degree of Al-Si disorder of the Mont St-Hilaire sodalite and sodalite synthesized at 8 kbar and 1173 K was evaluated by D. A. Howell at the University of Illinois using $^{29}Si$ nuclear magnetic resonance spectroscopy. Neither the natural nor synthetic sodalite show any evidence of Al-Si disorder.

Cell dimensions for selected sodalites and nephelines of this study were determined by J. E. Post at the Smithsonian Institution, with a smear mount on a quartz plate using an automated Scintag powder diffractometer with Cu-K$\alpha$ radiation. The measurements were made at 1°2$\theta$/min with an internal silicon standard (NBS 640-a). All data were processed with a least-squares lattice refinement program based on a minimum of six reflections (Table 2). The calculated cell parameters of the Mont St-Hilaire sodalite are nearly identical to those

of PETERSON (1983) [$a = 8.877(2)$] for sodalite from the same locality.

Nepheline was synthesized by decomposing the Mont St-Hilaire sodalite in a platinum crucible at 1623 K for 7 hours, followed by annealing at 1373 K for 13 hours and by reacting sodalite to nepheline + NaCl ($s$) in a sealed platinum capsule at 1323 K and 20 kbar confining pressure. The nepheline synthesized at 1 bar has a slightly greater volume than the nepheline synthesized at high pressure (Table 2). The dependence of nepheline cell parameters on its thermal history has been observed previously (SMITH and TUTTLE, 1957; DONNAY et al., 1959; HENDERSON and ROUX, 1976, 1977). After a high-pressure experiment, the cell parameters of nepheline are independent of the initial synthesis technique of the nepheline starting material. For most experiments the nepheline prepared by decomposing sodalite at 1 atm was used. The NaCl used in the experiments was Fisher Reagent Grade.

## Experimental method

The stability of sodalite as defined by reaction (1) was determined at 1 bar and at elevated pressures. Equal masses of sodalite and nepheline with excess NaCl were loaded into platinum sample capsules, dried at 383 K for 30 minutes and promptly sealed. The excess NaCl was added to all sample runs to insure that $a$(NaCl) = 1. Starting materials and experimental products were examined optically as well as by X-ray diffraction and microprobe (Tables 1 and 2). A variation of 30% or more in the integrated intensities in the X-ray patterns of sodalite or nepheline comprised a half reversal. Most reactions went to completion.

One-atmosphere experiments were conducted in a platinum-wound vertical quench furnace at the Geophysical Laboratory. The sample capsules were hung adjacent to a $Pt_{100}$-$Pt_{90}Rh_{10}$ thermocouple monitored by a Newport digital thermometer and suspended vertically in the furnace. All samples were drop-quenched into water. Variations in temperature were less than ±3°C at the thermocouple junction; the thermocouple was calibrated based on the melting point of gold (1336.15 K). A total of 22 runs were made.

The high-pressure experiments were conducted in the piston/cylinder apparatus of SRB at Stony Brook and later at the USGS, Menlo Park, with a 2.54 cm diameter NaCl-graphite furnace based on the design of JOHANNES (1978) as modified by BOHLEN (1984). All experiments were conducted with the "hot piston-in" method (MIRWALD et al., 1975; JOHANNES, 1978; BOHLEN, 1984). Temperatures were measured with a $Pt_{100}$-$Pt_{90}Rh_{10}$ thermocouple abutting the platinum sample capsule and were monitored by a room-temperature compensated digital thermometer. No correction was made for effects of pressure on the thermocouple. Temperature variations were less than ±3°C, and absolute temperature variations across the platinum capsule were less than ±5°C (BOHLEN, 1984). Pressures were measured with a digital Heise gauge; variations were less than 0.1 kbar. A total of 29 runs were made.

## EXPERIMENTAL RESULTS

### One atmosphere

The 1 atm breakdown temperature of sodalite to carnegieite (the high-temperature $NaAlSiO_4$ polymorph) and NaCl (liquid) was reversed between 1649–1652 K (Table 3). These data are in good agreement with the experimental determinations of WELLMAN (1969a) (1657–1667 K) and DEMIDENKO et al. (1983) (>1623 K), but far higher than those of TOMISAKA and EUGSTER (1968) (1503 ± 5 K).

### High pressure

The breakdown of sodalite to β-nepheline and halite (reaction [1]) was reversed at 923 K (7.6–8.0 kbar), 973 K (7.4–7.6 kbar), 1073 K (7.8–8.0 kbar) and 1173 K (8.4–8.6 kbar) (Table 3). Reaction rates at all temperatures were relatively rapid, even though all runs were anhydrous. The NaCl

Table 3. Critical experimental results for sodalite decomposition in the 1 bar vertical quench (VQ) furnace and at pressures using the piston/cylinder (PC) apparatus. (sod - sodalite, cg - carnegieite, ne - nepheline)

| Expt # | Temp. (K) | Pressure (kbar) | Duration (hrs) | Starting materials | Results |
|--------|-----------|-----------------|----------------|--------------------|---------|
| VQ-3 | 1644 | 0.001 | 3 | sod, cg, NaCl | sod, NaCl |
| VQ-5 | 1649 | 0.001 | 6 | sod, cg, NaCl | sod, NaCl |
| VQ-6 | 1652 | 0.001 | 12 | sod, cg, NaCl | cg, NaCl |
| PC-964 | 923 | 7.6 | 185 | sod, ne, NaCl | sod, NaCl trace ne |
| PC-971 | 923 | 8.0 | 120 | sod, ne, NaCl | ne, NaCl minor sod |
| PC-26 | 973 | 7.4 | 144 | sod, ne, NaCl | sod, NaCl |
| PC-18 | 973 | 7.6 | 144 | sod, ne, NaCl | ne, NaCl |
| PC-11 | 1073 | 7.8 | 41 | sod, ne, NaCl | sod, NaCl |
| PC-8 | 1073 | 8.0 | 22 | sod, ne, NaCl | ne, NaCl trace sod |
| PC-15 | 1173 | 8.0 | 21 | sod, ne, NaCl | sod, NaCl |
| PC-16 | 1173 | 8.4 | 23 | sod, ne, NaCl | sod, NaCl trace ne |
| PC-17 | 1173 | 8.6 | 23 | sod, ne, NaCl | ne, NaCl trace sod |
| PC-7 | 1173 | 10.0 | 22 | sod, ne, NaCl | ne, NaCl |

appears to act as a flux (as well as a reactant) to drive the reaction to completion. These reversals can be fit with a univariant line with a $dP/dT$ of +5 bar/K over the temperature interval 973–1173 K. However, the 923 K reversal requires a $dP/dT$ of −6 ± 6 bar/K between 973 K and 923 K.

## THERMODYNAMIC DATA IN THE SYSTEM $NaAlSiO_4$-NaCl

Phases in the system $NaAlSiO_4$-NaCl include $NaAlSiO_4$ polymorphs, halite, liquid NaCl and sodalite. In order to calculate the complete phase diagram for this system, accurate values of entropy ($S_{298}^0$ and $S_T^0$), volume ($V_{298}^0$), thermal expansion, compressibility and free energy are needed.

### NaCl

All of the necessary thermodynamic properties are available for NaCl ($s$) and NaCl ($l$) except for the compressibility of NaCl ($l$). The compressibility coefficients ($m$ and $n$ in Eqn. (4) for NaCl ($l$) were adjusted to fit the high-pressure experiments on the melting of NaCl (CLARK, 1959; BOHLEN, 1984) based on the following set of equations:

$$-\Delta G_{298}^{1\text{ bar}} = \int_{1\text{ bar}}^{P} \Delta V dP - \int_{298}^{T} \Delta S dT \qquad (2)$$

where

$$V(P, T) = V_{298}^0 [1 + A(T)][1 + B(P)]. \qquad (3)$$

The functions $A$ and $B$ are related to the expansivity $\alpha$ and compressibility $\beta$, respectively, and are represented by the following equations ($P$ in kbar; $T$ in K):

$$B(P) = -m \cdot 10^{-3} \cdot P + n \cdot 10^{-6} \cdot P^2 \qquad (4)$$

and

$$A(T) = \{e \cdot 10^{-2} + f \cdot 10^{-3} \cdot (T - 273) + g \cdot 10^{-7}$$

$$\times (T - 273)^2 + h \cdot 10^{-10} \cdot (T - 273)^3\}/100. \qquad (5)$$

All thermodynamic data are presented in Table 4.

### $NaAlSiO_4$

All thermodynamic data for the $NaAlSiO_4$ polymorphs needed in this study have been measured, except for the low-

Z. D. Sharp *et al.*

Table 4. Thermodynamic data of minerals used in for calculated equilibria.
S in J/mol K, ΔG in kJ/mol, V in cm³, T in K, P in kbar

| | $S^{\circ}_{298}$ | ref | a | b | c | d | ref | $\Delta G^{\circ}_{298}$ | ref |
|---|---|---|---|---|---|---|---|---|---|
| α-cg | 129.6 | (1) | 133.48 | 61.56 | 17.65 | -797.99 | (2) | -1958 | (1) |
| β-cg[1] | 129.6 | (1) | 178.95 | 5.87 | -7.28 | -1045.28 | (2) | -1963 | (1) |
| NaCl (s) | 72.12 | (3) | 35.94 | 27.51 | -5.38 | -207.92 | (3) | -384.02 | (3) |
| NaCl (l) | 95.06 | (3) | 65.44 | 4.07 | 12.47 | -387.46 | (3) | -365.67 | (3) |
| NaCl (v) | 229.69 | (3) | 37.35 | 0.73 | 0.83 | -214.35 | (3) | -201.33 | (8) |
| β-ne | 124.35 | (4) | 108.24 | 62.27 | -16.25 | -625.82 | (4,5) | -1977.5 | (5) |
| γ-ne[2] | 125.5 | (6) | 145.72 | 25.17 | 14.62 | -848.87 | (4) | -2137 | (4) |
| sod | 909.8 | (7) | 909.81 | 305.49 | 92.75 | -5421.44 | (7) | -1269/3 | (1) |

Entropy: $S^{\circ}_T$ $S^{\circ}_{298} = a \cdot \ln T + b \cdot 10^{-3} T + c \cdot 10^5 T^{-2} + d$

| | $V^{\circ}_{298}$ | ref | e | f | g | h | ref | m | n | ref |
|---|---|---|---|---|---|---|---|---|---|---|
| α-cg | 55.6 | (8) | -83.84 | 6.78 | -11.45 | 3.44 | (9) | 2.63 | 11.83 | (10) |
| β-cg[1] | 57.0 | (11) | -83.84 | 6.78 | -11.45 | 3.44 | (9) | 2.63 | 11.83 | (10) |
| NaCl (s) | 27.02 | (4) | -17.15 | 10.23 | 100.92 | -32.82 | (13) | 4.15 | 40.54 | (14) |
| NaCl (l) | 31.6 | (15) | -188.72 | 17.78 | 82.57 | 27.57 | (16) | 24.7 | 800 | (1) |
| β-ne | 54.18 | (17) | -59.38 | 2.56 | 38.06 | -14.89 | (17) | 2.06 | 4.89 | (14) |
| γ-ne[2] | 54.9 | (18) | 0.00 | 4.73 | 0.00 | 0.00 | (17) | 2.06 | 4.89 | (14) |
| sod | 421.3 | (19) | 0.33 | 1.96 | 51.08 | -15.73 | (20) | 1.76 | 0.00 | (21) |

Volume: $V^{\circ}_T = V^{\circ}_{298} + V^{\circ}_{298}[e \cdot 10^{-2} + f \cdot 10^{-5}(T - 273) + g \cdot 10^{-7}(T - 273)^2 + h \cdot 10^{-10}(T - 273)^3]/100;$

$V^P_{298} = V^{\circ}_{298}[1 - m \cdot 10^{-3} \cdot P + n \cdot 10^{-6} \cdot P^2]$

[1]valid above 960 K transition; [2]valid above 1133 K transition;
[3]excluding excess entropy contribution (61.7 J/mol·K) below 973 K.

Abbreviations: NaCl (s) = solid NaCl; NaCl (l) = NaCl liquid;
NaCl (v) = NaCl vapor; sod = sodalite.

1) Estimated, this study; 2) Kelley et al., 1953; 3) Chase et al., 1985;
4) Robie et al., 1978; 5) Henderson and Thompson, 1980; 6) Used value for
β nepheline; 7) Helffrich et al., 1986; Komada et al., 1989 with excess
entropy term included; 8) Klingenberg and Felscher (1981); 9) Extrapolated
high T data of Hummel, 1949; 10) Cristobalite data from Robinson et al.,
1982; 11) Extrapolated value of Smith and Tuttle, 1957; 12) Hummel, 1949;
13) Skinner, 1966; 14) Birch, 1966; 15) Extrapolated high T data of Janz,
1967; 16) Janz, 1967; 17) Henderson and Roux, 1977; 18) Extrapolated high T
data of Henderson and Roux, 1977; 19) This study; 20) Henderson and Taylor,
1978; 21) Hazen and Sharp, 1988.

temperature heat capacity of carnegieite (stable above 1525 K) and the compressibility of carnegieite and γ-nepheline (the nepheline polymorph stable above 1180 K and below 1525 K; KELLEY *et al.*, 1953). The thermal expansion of γ-nepheline has been measured (HENDERSON and ROUX, 1976, 1977), but only over a narrow temperature range. These thermodynamic properties were estimated in the following ways:

1. The entropy of carnegieite at 298 K was estimated from the following relation (FYFE *et al.*, 1958. p. 34):

$$S^0_{298}(cn) = S^0_{298}(ne) + 2.5 \, (J/mol \cdot K \cdot cm^3)$$

$$\times [V^0_{298}(cn) - V^0_{298}(ne)] \quad (6)$$

where cn = α-carnegieite and ne = α-nepheline (entropy in J/mol·K).

2. The compressibility of β- and γ-nepheline was assumed to be equal to that of α-nepheline. The actual compressibilities are probably slightly greater than this estimate (COHEN and KLEMENT, 1976), but small errors in this second-order term will not significantly alter the calculated equilibria.

3. The compressibility of carnegieite was assumed to be the same as that of isostructural cristobalite.

4. The thermal expansion of γ-nepheline and carnegieite were extrapolated linearly to temperatures of 1600 K and 1700 K, respectively, which may introduce small systematic errors.

### $Na_8Al_6Si_6O_{24}Cl_2$

The heat capacity of Mont St-Hilaire sodalite with a composition of $K_{0.01}Na_{7.99}Al_{6.00}Si_{5.96}Fe^{3+}_{0.04}O_{23.98}Cl_{1.96}(SO_4)_{0.02}$

(HELFFRICH *et al.*, 1986) has been measured with low-temperature (15–350 K) adiabatic calorimetry and high-temperature (298.15–1000 K) differential scanning calorimetry (HELFFRICH *et al.*, 1986; KOMADA *et al.*, 1989). The heat capacity of end-member sodalite ($Na_8Al_6Si_6O_{24}Cl_2$) was estimated by correcting for the effects of minor element substitution and contamination by fluid inclusions. The corrected value of $S^0_{298}$-$S^0_0$, 848.1 ± 4.0 J/mol·K, is intermediate between earlier estimates of 814 ± 30 J/mol·K (SEMENOV *et al.*, 1981) and 879 ± 25 J/mol·K (ZOLOTOV *et al.*, 1982). The large uncertainty in the earlier estimates may result from those earlier heat capacity measurements being made only above 77 K.

As a result of the high thermal stability of sodalite, data for thermal expansion and entropy of sodalite are needed to 1700 K. Thermal expansion has only a small effect on the calculated phase relations, and graphical extrapolation of the volume ($V^0_T$) of sodalite (measured to 1078 K) to 1700 K should not result in significant errors. However, the effect of temperature on the entropy of sodalite will affect its calculated stability relations, and extrapolation of the entropy of sodalite over a large temperature range cannot be made without the risk of introducing serious errors. The procedure outlined below was used to extrapolate the entropy of sodalite (measured to 1000 K) to 1700 K.

As a first approximation, the entropy of a solid phase is equal to the sum of its components (*e.g.*, FYFE *et al.*, 1958; WOOD and FRASER, 1977; HELGESON *et al.*, 1978). The entropy of sodalite at high temperature can be approximated from the relation

$$S^0_T(sod) \approx 6 \, S^0_T(NaAlSiO_4) + 2 \, S^0_T(NaCl)(s). \quad (7)$$

Because β-nepheline is stable only to 1133 K at 1 bar, entropy data above this temperature cannot be measured at 1 bar, and the substitution of β-nepheline for Eqn. (7) is not useful for determining the entropy of sodalite above 1133 K. Instead, the entropy of sodalite at high temperatures was estimated by substituting the entrophy values of γ-nepheline, carnegieite and a fictive $NaAlSiO_4$ component (ROBINSON and HAAS, 1983) into Eqn. (7). The entropy difference ($\Delta S_{calc-meas}$) is nearly linear between 500 K and 1000 K when the fictive $NaAlSiO_4$ entropy value is used. The $\Delta S_{calc-meas}$ was linearly extrapolated to 1700 K. The entropy of sodalite above 1000 K was then estimated by adding the $\Delta S_{calc-meas}$ to the sums of the entropies of fictive $NaAlSiO_4$ and NaCl (*s*) from Eqn. (3). Entropy data for NaCl (*s*) are available to 1500 K (CHASE *et al.*, 1985) and were extrapolated graphically to 1700 K in order to make the above calculation. The uncertainty in the entropy of sodalite at 1700 K is estimated to be less than 2%.

### SELECTED PHASE EQUILIBRIA IN THE SYSTEM $NaAlSiO_4$-$SiO_2$-NaCl

*NaCl*

Melting relations for NaCl have been well constrained as a function of pressure and temperature (CLARK, 1959; BOHLEN, 1984). The calculated melting equilibria from the data in Table 4 reproduce the melting experiments (Fig. 1a,b), because the compressibility of NaCl liquid was obtained from
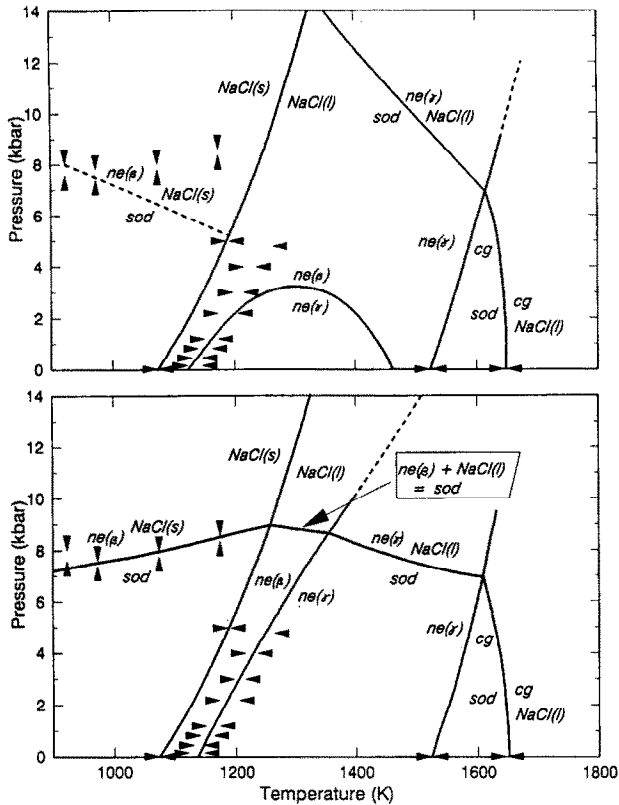
FIG. 1. Selected stability relations of phases in the system $NaAlSiO_4$-$SiO_2$-NaCl. Reversals (triangles) as follows: $ne(\beta)$ + NaCl (s) = sod (this study); $ne(\beta)$ = $ne(\gamma)$ (COHEN and KLEMENT, 1976); NaCl (s) = NaCl (l) (BOHLEN, 1984); $ne(\gamma)$ = cg (BOWEN, 1912; KELLEY et al., 1953; SMITH and TUTTLE, 1957); sod = cg + NaCl (l) (this study; at 1649–1652 K). (Abbreviations: cg = carnegieite, ne = nepheline, sod = sodalite). Figure 1a is generated with the measured $S^0_{298}$ of sodalite. The sodalite-bearing reactions are constrained by the 1 bar, 1649–1652 K reversal except for the dashed line for reaction (9), which is fit to the 923 and 973 K, high-pressure reversal. A phase diagram cannot be generated that is consistent with both sets of experiments. Figure 1b includes an excess entropy term for sodalite of 61.7 J/mol · K. The generated curves coincide with all experiments above 973 K. The excess entropy contribution is only required above 923 K.

the experimental curves. The boiling point of NaCl at 1 bar is 1791 K (ROBIE et al., 1978), well above the stability of sodalite. At pressures below 1 bar, NaCl (s), NaCl (l) or NaCl (v) will coexist with sodalite (e.g., WELLMAN, 1969b). The stability fields of NaCl (s), NaCl (l) and NaCl (v) at reduced NaCl fugacities (Fig. 2a,b) were calculated from the data in Table 4.

## NaAlSiO4

$NaAlSiO_4$ is a complex phase with at least six polymorphs. The stabilities and structural transformations of these polymorphs have received considerable attention (BOWEN, 1912; BOWEN and GREIG, 1925; KELLEY et al., 1953; SMITH and TUTTLE, 1957; TUTTLE and SMITH, 1958; DONNAY et al., 1959; ROY and ROY, 1969; COHEN and KLEMENT, 1976; HENDERSON and ROUX, 1977; HENDERSON and THOMPSON, 1980). The low-temperature polymorph of $NaAlSiO_4$ un-

dergoes two known inversions at 1 bar. The high-temperature polymorph, carnegieite, has a metastable transition in the stability field of nepheline. Additional polymorphism has been proposed at ultra-high pressures (synthesized at 180 kbar and 1273 K, LIU, 1977; 58 kbar and 1673 K, SHANNON and BERZINS, 1979), and possibly at moderate temperature and pressure (443 K, 2–3 kbar, COHEN and KLEMENT, 1976).

The lowest temperature transition in nepheline ($\alpha$-$\beta$) is second or higher order (McCONNELL, 1981), and occurs over a temperature range of at least 416–469 K. The higher temperature nepheline inversion ($\beta$-$\gamma$) is complex, and may be a combination of first- and second-order behavior. The $\beta$-$\gamma$ nepheline transition occurs over the temperature interval 1083–1233 K (1180 K, KELLEY et al., 1953; 1123–1173 K, TUTTLE and SMITH, 1958; 1083 K, DONNAY et al., 1959; 1148–1198 K, ROY and ROY, 1969; 1118–1145 K, COHEN and KLEMENT, 1976; 1148–1233 K, HENDERSON and ROUX, 1977). The breakdown of nepheline to carnegieite is sluggish and occurs between 1521–1525 K. The high-temperature phase, carnegieite, is quenchable, although it undergoes a
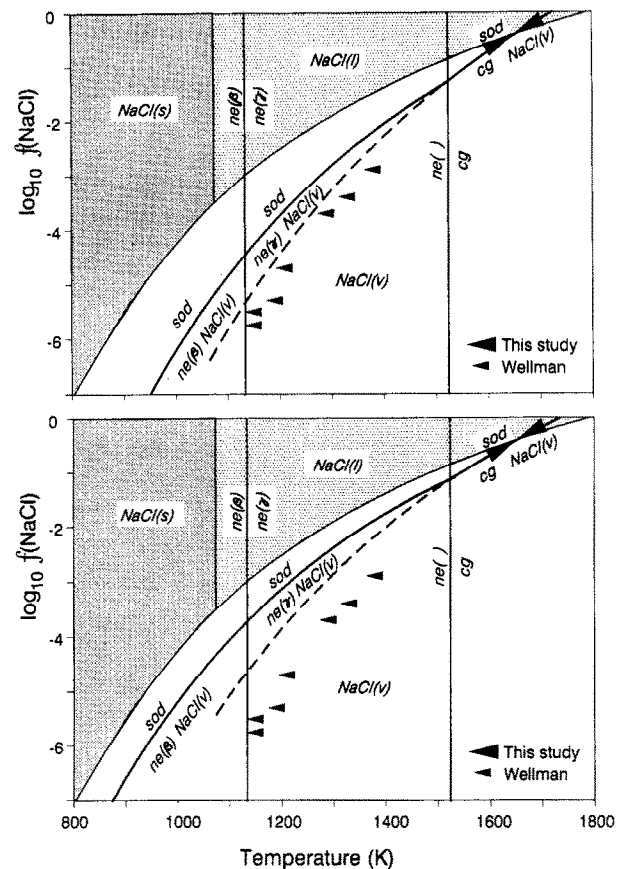


FIG. 2. Stability fields of NaCl (s), NaCl (l), NaCl (v) and sodalite at various NaCl fugacities. Experiments of WELLMAN (1969b) are for reaction (19). The location of the sodalite stability curves is based on the reversal from this study (1649–1652 K) for reaction (12) at the intersection with the NaCl (l) = NaCl (v) equilibria. Dashed line is the metastable extension of sod = cg + NaCl (v) in the nepheline stability field. Figure 2a is generated with the measured $S^0_{298}$ of sodalite; Figure 2b includes an excess entropy contribution of 61.7 J/ mol · K. Abbreviations as in Fig. 1.

metastable, rapid inversion ($\alpha$-$\beta$) between 944–980 K. The temperature of this inversion depends on the thermal history of the sample (COHEN and KLEMENT, 1976). Only the $\beta$-$\gamma$ nepheline inversion and the $\gamma$-nepheline-carnegieite reaction directly affect the stability field of sodalite in the *P-T* range of this study. The entropy contributions of the low-temperature nepheline inversion and the $\alpha$-$\beta$ carnegieite transition are included in the entropy values of the stable phases at higher temperature.

COHEN and KLEMENT (1976) determined the temperature of the $\beta$-$\gamma$ nepheline transition at pressures of 1 bar to 5 kbar; it occurs at approximately 1133 K at 1 bar and has a $dP/dT$ of 42 bar/K. At temperatures up to 1200 K the $\beta$-$\gamma$ transition can be fit with available thermodynamic data. With increasing temperature, the calculated $dP/dT$ decreases and eventually becomes negative, so that $\beta$-nepheline is apparently again stable at 1 bar ($\sim$1450 K) (Fig. 1a). This unusual result occurs because the entropy of $\beta$-nepheline, graphically extrapolated into the $\gamma$-nepheline stability field, becomes greater than that of $\gamma$-nepheline. If the measured heat capacity and integrated entropy data for $\beta$- and $\gamma$-nepheline are correct, then the computed stability of $\beta$-nepheline must lie both below and above that of $\gamma$-nepheline at 1 bar. The same apparent relationship is encountered across other mixed-order phase transitions, such as $\alpha$-quartz/$\beta$-quartz. The explanation for these unlikely stability relations is likely associated with either 1) errors in the extrapolation of the entropy of $\beta$-nepheline into the $\gamma$-nepheline stability field at 1 bar, or 2) errors in the extrapolation of 1 bar entropy values to higher pressures.

The thermodynamics of second- and higher-order transitions become complex as conventional thermodynamic relationships become indeterminate (*e.g.*, THOMPSON and PERKINS, 1981). It is possible that heat capacity contributions associated with the transition, which occur over a 100–200°C temperature interval below the actual transition, are being measured. If this effect is not taken into account, the $\Delta S$ associated with the phase transition will be smeared out over a large temperature interval, and will appear too small. The effects of pressure on these complex transitions is not known, but the enthalpy and entropy changes across transitions in simple salts are reduced with increasing pressure (WESTRUM, 1974). In the present calculations, the effect of pressure on entropy is accounted for by the relationship
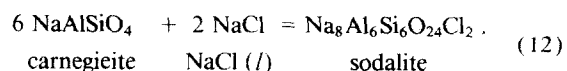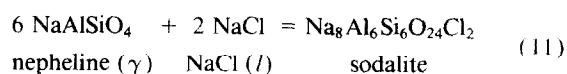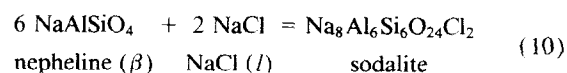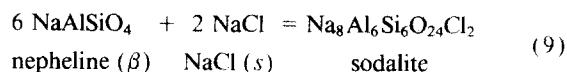
$$(\partial S/\partial P)_T = -\alpha V. \qquad (8)$$

where $\alpha$ = thermal expansion. However, this expression may not adequately account for other unknown pressure effects associated with complex high-order polymorphic transitions. In this study, the $\beta$-$\gamma$ nepheline transition was fit by forcing the extrapolated 1 bar entropy values of $\beta$-nepheline in the $\gamma$-nepheline field to be less than those measured for $\gamma$-nepheline.

The transition temperature for the nepheline-carnegieite inversion is well documented at 1 bar but has not been determined at higher pressures. The calculated $dP/dT$ of this reaction (70 bar/K) determined with available thermodynamic data is poorly constrained because of the small $\Delta V$ and $\Delta S$ for this reaction and the uncertainties in the high-temperature thermodynamic data for $\gamma$-nepheline and carnegieite. However, a consistent set of thermodynamic data

in the NaAlSiO-NaCl system, constrained by the nepheline-carnegieite and sodalite decomposition equilibria is generated when the $S^0_{298}$ of carnegieite (Table 4) is assumed to be 1.7 J/mol·K (1.3%) greater than the calculated value of 127.9 J/mol·K from Eqn. (6). Under these conditions the $dP/dT$ for the nepheline-carnegieite transition is 72 bar/K.

### NaAlSiO$_4$-NaCl

In order to calculate the stability of sodalite, the decomposition of sodalite by reaction (1) must be further subdivided into a series of reactions based on the stable phases for NaAlSiO$_4$ and NaCl. With increasing temperature, these reactions are as follows:

$$6\text{ NaAlSiO}_4 + 2\text{ NaCl} = \text{Na}_8\text{Al}_6\text{Si}_6\text{O}_{24}\text{Cl}_2 \qquad (9)$$

nepheline ($\beta$)      NaCl ($s$)           sodalite

$$6\text{ NaAlSiO}_4 + 2\text{ NaCl} = \text{Na}_8\text{Al}_6\text{Si}_6\text{O}_{24}\text{Cl}_2 \qquad (10)$$

nepheline ($\beta$)      NaCl ($l$)            sodalite

$$6\text{ NaAlSiO}_4 + 2\text{ NaCl} = \text{Na}_8\text{Al}_6\text{Si}_6\text{O}_{24}\text{Cl}_2 \qquad (11)$$

nepheline ($\gamma$)      NaCl ($l$)           sodalite

$$6\text{ NaAlSiO}_4 + 2\text{ NaCl} = \text{Na}_8\text{Al}_6\text{Si}_6\text{O}_{24}\text{Cl}_2 . \qquad (12)$$

carnegieite           NaCl ($l$)            sodalite

The slope for reaction (9), calculated from the available thermodynamic data for the phases $\beta$-nepheline, NaCl ($s$) and sodalite, is $-11.0$ bar/K between 973 and 1173 K, but the slope required to fit the experimental reversals is $+5$ bar/K in this temperature interval. The slope constrained by the 923 K and 973 K reversals is $6 \pm 6$ bar/K, consistent with the calculated slope for reaction (9). The discrepancy above 973 K is greater than the sum of the uncertainties in the entropy and volume data of sodalite, $\beta$-nepheline and NaCl ($s$). A fit to the high-pressure experimental reversals can be obtained if the entropy of sodalite is increased by 61.7 J/mol·K (7.3%) above 973 K. This entropy contribution could be due to configurational disorder, nonstoichiometry or a phase transition. Possible entropy contributions to nepheline or NaCl must be ruled out, because these adjustments would increase, rather than decrease, the misfit between calculated and experimental slopes of reaction (9).

The entropy contribution from complete configurational disorder between Al and Si over two tetrahedral sites is $12R$ ln 2, or 69.15 J/mol·K, where $R = 8.3143$ J/mol·K. The predicted value of 61.7 J/mol·K requires 58% disorder over 12 sites (where 100% = complete disorder). Other entropy contributions resulting from nonstoichiometry are possible, but extreme nonideality would be required to account for the large entropy contribution required to fit the experimental reversals.

Excess entropy predicted for sodalite from the experimentally determined slope of reaction (9) is not in agreement with other data on Cl-bearing sodalites. Structure refinements (LONS and SCHULZ, 1967; PETERSON, 1983) and infrared studies (HENDERSON and TAYLOR, 1979) of sodalite are consistent with total or near-total order of Al-Si. A [29]Si nuclear magnetic resonance study on the Mont St-Hilaire sodalite equilibrated at 1123 K/6 kbar was performed by D. A. Howell

in the Laboratory of Dr. J. R. Kirkpatrick at the University of Illinois, Urbana, and it shows no signs of Al-Si disorder (D. Howell, pers. commun.). This natural sample was held at elevated pressure and temperature, but was not synthesized from nepheline + NaCl. It is possible that sodalite rapidly synthesized from NaCl and nepheline may be disordered, as is ultramarine when pyrolitically synthesized from kaolin, sodium carbonate and sulfur (KLINOWSKI et al., 1987). Because there is a one to one ratio of tetrahedral Al and Si in sodalite, any disorder of Al-Si would violate the "aluminum avoidance principle" (LOEWENSTEIN, 1954). Yet ultramarine, which has the sodalite structure with sulfur as the cavity anion, exhibits total Al-Si disorder (KLINOWSKI et al., 1987), iodine sodalite ($Na_8(Al_6Si_6O_{24})I_2$) appears to have partial Al-Si disorder (BEAGLEY et al., 1982) and there is some suggestion of disorder in synthetic Rb-rich sodalite above 973 K (HASSAN and GRUNDY, 1984). Al-Si disorder could be responsible for the experimentally determined $dP/dT$ for reaction (9) above 973 K as well. The cell parameters of sodalite quenched from high temperatures are greater than the natural material (Table 2), consistent with this hypothesis. Moreover, the onset of disordering, $\sim$973 K, roughly agrees with the temperatures at which GOLDSMITH and JENKINS (1985) found Al-Si redistribution associated with the low- to high-albite transition (930 K). This transition, which involves Al-Si diffusion between vertex-connected tetrahedra, is facilitated by pressure, which may account for the lack of calorimetric evidence for the transition below 1000 K, the limit of the calorimetric data.

An alternative explanation for the discrepancy between the experimentally and thermodynamically determined stability fields for sodalite-bearing assemblages is that sodalite undergoes a reversible phase transition at elevated pressure and temperature. If this is the case, and the thermodynamic properties of this new phase are sufficiently different from sodalite, a consistent fit of the thermodynamic data to the reversals could be made without requiring configurational disorder.

The calculated stability relations of sodalite-bearing assemblages generated by an internally consistent set of thermodynamic data must pass through the reversals for Eqns. (9) and (12). It is not possible to derive a phase diagram for the system $NaAlSiO_4$-NaCl (Fig. 1a) using the measured thermodynamic database that is consistent with the experimental reversals from this study. However, agreement can be achieved if the entropy of sodalite above 923 K is increased by 61.7 J/mol·K and the $S^0_{298}$ of carnegieite is 1.7 J/mol·K greater than the estimate from Eqn. (6) (Fig. 1b).

### Aluminosilicate solid-solution in NaCl liquid

The experimentally determined NaCl ($l$)-bearing univariant equilibria will differ from the calculated ones if NaCl ($l$) is significantly diluted by solid-solution with dissolved aluminosilicate. In order to determine the degree of solid-solution of aluminum and silicon in NaCl ($l$), large sodalite crystals were equilibrated with NaCl at 1621 K for 19 hours in a sealed platinum capsule. The sample was quenched, the sodalite crystals were removed, and the salt was analyzed for Al and Si with the Jobin Yvon JY70 Type II inductively

coupled plasma-atomic emission spectrometer at the Geophysical Laboratory. Silicon is undetectable and aluminum has a concentration of <30 ppm. The effects of these small concentrations of Al and Si in NaCl on the calculated phase equilibria may be ignored.

### $NaAlSiO_4$-$SiO_2$-NaCl

Expanding the $NaAlSiO_4$-NaCl system to include $SiO_2$ adds the phases jadeite, albite and quartz along the $NaAlSiO_4$-$SiO_2$ join. The formation of jadeite (NEWTON and KENNEDY, 1968; BOETTCHER and WYLLIE, 1968) by the equilibrium

$$2\ NaAlSi_2O_6 = NaAlSiO_4 + NaAlSi_3O_8 \qquad (13)$$
$$\text{jadeite} \qquad\quad \text{nepheline} \qquad \text{albite}$$

can be combined with equilibrium (9) to generate

$$12\ NaAlSi_2O_6 + 2\ NaCl$$
$$\text{jadeite} \qquad\qquad \text{halite}$$

$$= Na_8Al_6Si_6O_{24}Cl_2 + 6\ NaAlSi_3O_8. \qquad (14)$$
$$\text{sodalite} \qquad\qquad \text{albite}$$

The formation of albite (HAYS and BELL, 1973) by the reaction

$$NaAlSi_3O_8 = NaAlSi_2O_6 + SiO_2 \qquad (15)$$
$$\text{albite} \qquad\quad \text{jadeite} \qquad \text{quartz}$$

can be combined with equilibrium (14) to generate two quartz-sodalite bearing reactions:

$$6\ NaAlSi_2O_6 + 2\ NaCl = Na_8Al_6Si_6O_{24}Cl_2 + 6\ SiO_2 \quad (16)$$
$$\text{jadeite} \qquad\quad \text{halite} \qquad\quad \text{sodalite} \qquad\qquad \text{quartz}$$

and

$$6\ NaAlSi_3O_8 + 2\ NaCl = Na_8Al_6Si_6O_{24}Cl_2 + 12\ SiO_2 \quad (17)$$
$$\text{albite} \qquad\quad \text{halite} \qquad\quad \text{sodalite} \qquad\qquad \text{quartz.}$$

The pressure and temperature at which reactions (9) and (13) intersect is dependent on the presumed high-pressure/temperature entropy of sodalite. If the slope of reaction (9) changes from +5 bar/K to −11 bar/K between 973 and 923 K, then the invariant point defined by reaction (9) and (13) occurs at 773 K and 10 kbar. If the excess entropy contribution to sodalite is included down to 298 K, the invariant point defined by reactions (9) and (13) occurs at 573 K and 5.5 kbar. In either case, the mutual stability of sodalite and jadeite will be reduced further if NaCl activity is less than 1. The stability field of quartz + sodalite, limited by reactions (16) and (17), lies at temperatures below 298 K. The equilibrium coexistence of natural sodalite and quartz or sodalite and jadeite has never been reported to our knowledge.

### Comparison with previous work

WELLMAN (1969b) determined the decomposition temperature of sodalite to γ-nepheline + NaCl ($v$). The data are shown in Fig. 2a and b along with the calculated equilibrium for the breakdown of sodalite by the equilibria

$$6\ NaAlSiO_4 + 2\ NaCl = Na_8Al_6Si_6O_{24}Cl_2 \qquad (18)$$
$$\text{γ-nepheline} \qquad \text{NaCl}\ (v) \qquad\qquad \text{sodalite}$$

and

$$6\ NaAlSiO_4 + 2\ NaCl\ =\ Na_8Al_6Si_6O_{24}Cl_2 \quad (19)$$

carnegieite    NaCl $(v)$         sodalite.

The decomposition data of WELLMAN (1969b) are most closely matched by the calculated equilibrium for reaction (19) excluding the excess entropy contribution to sodalite (Fig. 2a). Wellman was unable to reverse his decomposition reactions at low $f(NaCl)$ to form sodalite from halite and nepheline. Therefore, the experiments of Wellman represent "half reversals", and are equally consistent with all calculated sodalite-bearing equilibria in Fig. 2a and b.

The data of WELLMAN (1969b) are more closely matched by the metastable extension of reaction (19) than by reaction (18), and they suggest that sodalite decomposes metastably to carnegieite in the $\gamma$-nepheline stability field at pressures less than 1 bar (Fig. 2a,b). This assumption was tested by simulating the experimental conditions of WELLMAN (1969b) for sodalite decomposition at low $f(NaCl)$. Sodalite, loaded in an open platinum capsule in the end of a long evacuated silica tube, was placed into a horizontal furnace with a constant-temperature region in the center and a region of smoothly decreasing temperature toward the end. The sodalite-bearing end was positioned in the constant temperature region at 1250 K. The temperature at the cool end of the tube was lowered in 30 minute intervals by sliding the end of the tube away from the hot spot of the furnace until halite could be seen precipitating at the cool end. An X-ray determination of the reaction products confirmed that carnegieite is produced metastably under these conditions.

STORMER and CARMICHAEL (1971) calculated the free energy of sodalite at elevated temperatures assuming that the decomposition temperatures (WELLMAN, 1969b) represent equilibrium conditions for reaction (18) rather than reaction (19). In our study, the free energy of sodalite was calculated from the 973 K, 7.5 ± 0.1 kbar reversal for reaction (9) extrapolated to 1 bar at constant temperature using the equation

$$\Delta G_T^P - \Delta G_T^0 = \int_{1\ bar}^{P} \Delta V dP. \quad (20)$$

The free energy of sodalite at 1 bar was then calculated over a broad range of temperature by summing the entropy contributions of the elements as a function of temperature both with and without the excess entropy contribution for sodalite. At 1000 K, the free energy estimate of STORMER and CARMICHAEL (1971) is more negative, and at 1400 K, the estimate of Stormer and Carmichael is less negative than the present estimates (Table 5). This discrepancy is produced by their use of thermodynamic data for nepheline rather than carnegieite. The free energy of sodalite at 973 K, based on the enthalpy data of KOMADA *et al.* (1989), is slightly more negative than the present estimate (Table 5) and corresponds to an equilibrium pressure of 20 kbar at 973 K for reaction (9). The very different calculated stability field of sodalite based on the enthalpy data of KOMADA *et al.* (1989) illustrates the sensitivity of solid-solid reactions to even small differences in free energy estimates.

Table 5. Gibbs free energy of sodalite, $(Na_8Al_6Si_6O_{24}Cl_2)$ in kJ/mol. Data from this study are based on the 973 K, 7.5 kbar reversal for reaction (9) with and without excess entropy term (E.E.) of 61.7 J/mol·K; data from Stormer & Carmichael (1971) (S & C) are based on stability experiments of Wellman (1969b) for reaction (17); data from Komada et al. (1989) are based on enthalpy measurements.

| T (K) | This study w/o E.E. | This study w/ E.E. | S & C. | Komada |
|---|---|---|---|---|
| 298 | -12696.5 | -12654.9 | -- | -- |
| 973 | -10963.8 | -10963.8 | -11000.4[1] | -11018.7 |
| 1000 | -10893.6 | -10895.3 | -10926.9 | -- |
| 1100 | -10635.1 | -10643.2 | -10656.6 | -- |
| 1200 | -10362.1 | -10375.9 | -10373.0 | -- |
| 1300 | -10042.4 | -10061.2 | -10040.8 | -- |
| 1400 | -9726.1 | -9749.0 | -9708.6 | -- |
| 1500 | -9412.7 | -9439.1 | -- | -- |

[1]extrapolated.

## GEOLOGICAL APPLICATIONS

### NaCl activities in undersaturated magmas

Sodalite is stable over a broad temperature range, and its presence can be used to constrain the activity of NaCl in a nepheline-bearing magma. Sodalite is found as euhedral phenocrysts at Mont St-Hilaire, with a coarsely crystalline groundmass of perthitic potassium feldspar, aegirine, nepheline and minor niobium-rich astrophyllite with late-stage albite. Additional late, minor phases, identified with BSE and EDA on the electron microprobe, include serandite, kupletskite, ferroan sphalerite, thorite, elpidite, catapleiite, a mineral of the bastnaesite-synchysite group, thorite and a rare-earth calcium phosphate (cheralite?). In order to calculate activities of NaCl in the Mont St-Hilaire syenite, estimates of the temperature, pressure and nepheline activity during sodalite crystallization must be made.

Pressure estimates for the Mont St-Hilaire complex are approximately 1 kbar, based on stratigraphic relationships (CURRIE *et al.*, 1986). No direct temperature estimates have been made on the sodalite-bearing syenites from Mont St-Hilaire. However, crystallization experiments of a sodalite-bearing naujaite from Ilímaussaq, Greenland (PIOTROWSKI and EDGAR, 1970) show that sodalite is the first phase to crystallize (1460 K at 1 atm, 1168 K at 1 kbar water pressure), and melting experiments in the system $NaAlSiO_4$-$SiO_4$-$NaCl$-$H_2O$ at 1 kbar indicate that temperatures greater than 1073 K are required to generate a liquid in the presence of sodalite (BARKER, 1976). Homogenization temperatures of fluid inclusions in nepheline from the sodalite-naujaite from Ilímaussaq are 1123–1313 K (SOBOLEV *et al.*, 1970). All of these data, based on similar rock types, are consistent with high crystallization temperatures in the range of 1073–1300 K for sodalite-bearing rocks.

The nepheline activity in the Mont St-Hilaire sodalite syenite was set equal to the measured ratio of $Na/(Na + K)$ = 0.83 in the nepheline. This is based on the assumptions that nepheline composition-activity relations are ideal over the solid solution interval $NaAlSiO_4$-$Na_{0.75}K_{0.25}AlSiO_4$ and that the measured nepheline composition at Mont St-Hilaire has not changed following crystallization. Minimum NaCl activities of the melt are 0.05 at 1073 K and 0.13 at 1273 K. As the magma cooled, a highly saline fluid would be evolved (*cf.*, KILINC and BURNHAM, 1972), and NaCl, which is

strongly partitioned into the aqueous phase, would be removed from the silicate melt. Evidence of this NaCl-rich aqueous fluid is preserved in fluid inclusions with halite daughter salts and salinities of 30 wt% (F. M. Haynes, pers. commun.).

During the crystallization of a syenitic magma, the NaCl concentration of the magma and any corresponding fluid phase will change. Crystallization of albite from an albite-rich, NaCl-$H_2O$-bearing liquid will lead to an increasing concentration of NaCl and $H_2O$ in the liquid until a $H_2O$-NaCl-rich fluid (or vapor) develops (KOSTER VAN GROOS and WYLLIE, 1969). In the case of an undersaturated bulk composition with a sufficiently high NaCl content, sodalite will be the first phase to crystallize (BARKER, 1976), leading to a depletion in the NaCl content of the residual magma. This will continue until nepheline begins to crystallize. As long as both sodalite and nepheline are present and in equilibrium, the NaCl activity of the magma will be buffered by reactions (9–12). The NaCl activity can be calculated from the sodalite-nepheline buffer, but the fluid salinities during the early stages of crystallization may only be determined if accurate activity-salinity relationships at elevated pressure and temperatures are known or if primary fluid inclusions in sodalite formed and are preserved. Unfortunately, the fluid inclusions in the Mont St-Hilaire sodalite are secondary, and no comparison of the fluid salinities from these inclusions and NaCl activities at the temperature of sodalite growth can be made.

### Sodalite as an NaCl buffer in experiments at high pressure and temperatures

Because sodalite is stable at very high temperatures, it may be used as a buffer in experimental studies of siliceous melts. A wide miscibility gap exists between NaCl-rich liquids and silicate liquids (e.g., KOSTER VAN GROOS and WYLLIE, 1969). The NaCl activities will be equal in a melt coexisting with a NaCl-saturated aqueous solution, so unit melt activities can be achieved by saturation of NaCl in the aqueous solution. If sodalite phenocrysts were present in a siliceous melt co-

existing with a NaCl-saturated aqueous fluid, the activity of $NaAlSiO_4$ will be buffered by reaction (1) and can be uniquely determined from the thermodynamic data in Table 4. This buffer may prove useful in studies of species activity in appropriate silicate liquids.

### Buoyancy of sodalite in magmas

As a result of its large open framework structure, the density of sodalite is very low. Sodalite is found as phenocrysts in the upper levels of the Mont St-Hilaire syenite, in the Ilímaussaq sodalite-syenites, South Greenland (USSING, 1912; SÖRENSEN, 1958) and in the Lovozero intrusion, Kola Peninsula, West Soviet Union (VLASOV et al., 1966). The stratification of the sodalite-bearing layers at Ilímaussaq has been attributed to sodalite flotation (USSING, 1912, p. 352). Studies of liquid and crystal densities will permit evaluation of crystal flotation under a variety of conditions (e.g., BOTTINGA and WEILL, 1970; CAMPBELL et al., 1978; STOLPER et al., 1981; IRVINE, 1987). Sodalite buoyancy could explain the stratification in these large alkali intrusions and also the local reverse zonation (downward enrichment) of silica in the Ilímaussaq and Lovozero intrusions. In order to test this hypothesis, the density of both the sodalite and the magma must be known under the conditions of sodalite crystallization, and the viscosity of the magma must be estimated to calculate rates of sodalite removal by flotation.

Direct density measurements were made on 5 g of Mont St-Hilaire sodalite in a Berman balance with toluene as the immersion fluid. The measured density, 2.276(5) g/cm$^3$, is identical to the calculated value of 2.276 from a molecular weight of 959.7 g/mol from the sodalite analysis of the Mont St-Hilaire sodalite (Table 1) and a unit cell volume of 421.56 cm$^3$/mol (Table 2). The density of sodalite can be calculated at elevated temperatures by combining the high-temperature volume data of HENDERSON and TAYLOR (1978) with the room temperature density determination. In order to determine the density of the melt coexisting with sodalite, the composition of the melt must be estimated. The melt com-

Table 7. Sodalite density and melt densities for anhydrous and hydrous conditions. Data in gm/cm³. BWR = Bottinga et al. (1982); L&C = Lange and Carmichael (1987).

| | sodalite | melt | | | melt | | | melt | | |
|---|---|---|---|---|---|---|---|---|---|---|
| | | Mont St-Hilaire | | | Ilimaussaq | | | Lovozero | | |
| | BWR | BWR | L&C | L&C | BWR | L&C | L&C | BWR | L&C | L&C |
| | | water content wt % | | | water content wt % | | | water content wt % | | |
| T(K) | 0.00 | 0.00 | 0.00 | 4.26 | 0.00 | 0.00 | 2.52 | 0.00 | 0.00 | 1.48 |
| 1000 | 2.23 | 2.49 | 2.56 | 2.34 | 2.60 | 2.70 | 2.54 | 2.68 | 2.71 | 2.62 |
| 1200 | 2.21 | 2.46 | 2.53 | 2.26 | 2.55 | 2.65 | 2.47 | 2.63 | 2.67 | 2.55 |
| 1400 | 2.18 | 2.43 | 2.51 | 2.19 | 2.50 | 2.61 | 2.39 | 2.58 | 2.63 | 2.49 |
| 1600 | 2.16 | 2.40 | 2.48 | 2.11 | 2.45 | 2.57 | 2.32 | 2.53 | 2.59 | 2.43 |

Table 6. Chemical compositions of sodalite-bearing syenites from Mont St-Hilaire (This study; XRF), Ilimaussaq (Hamilton, 1964; wet chemical) and Lovozero (Vlasov et al., 1966; wet chemical), and calculated groundmass composition less sodalite. Groundmass compositions are calculated for both anhydrous and hydrous conditions assuming that the water content of the melt is equal to the water content of the analysis. Groundmass compositions from Mont St-Hilaire are calculated assuming a whole rock chlorine content 0.3 wt % less than measured by the XRF analysis, as suggested by the wet chemical analysis. (WR = whole rock; LOI = loss on ignition; n.d. = not determined).

| | Mont St-Hilaire | | | Ilimaussaq | | | Lovozero | | |
|---|---|---|---|---|---|---|---|---|---|
| | WR | Groundmass (water content) | | WR | Groundmass (water content) | | WR | Groundmass (water content) | |
| | | 0.0 | 3.73* | | 0.0 | 2.52 | | 0.0 | 1.48 |
| SiO2 | 47.20 | 63.32 | 60.96 | 46.82 | 54.59 | 53.21 | 47.57 | 54.16 | 53.36 |
| TiO2 | 0.05 | 0.13 | 0.12 | 0.30 | 0.51 | 0.50 | 0.44 | 0.70 | 0.69 |
| ZrO2 | n.d. | n.d. | n.d. | 0.41 | 0.70 | 0.68 | 0.37 | 0.59 | 0.58 |
| Al2O3 | 26.40 | 19.41 | 18.69 | 22.42 | 16.87 | 16.44 | 21.90 | 16.45 | 16.21 |
| Fe2O3 | 1.23 | 3.09 | 2.98 | 3.00 | 5.11 | 4.98 | 5.18 | 8.28 | 8.15 |
| FeO | n.d. | n.d. | n.d. | 2.10 | 3.57 | 3.48 | 0.85 | 1.36 | 1.34 |
| MnO | 0.12 | 0.30 | 0.29 | 0.13 | 0.22 | 0.22 | 0.38 | 0.61 | 0.60 |
| MgO | 0.06 | 0.15 | 0.15 | 0.16 | 0.27 | 0.27 | 0.34 | 0.54 | 0.54 |
| CaO | 0.21 | 0.53 | 0.51 | 1.24 | 2.11 | 2.06 | 0.66 | 1.05 | 1.04 |
| Na2O | 17.70 | 6.44 | 6.20 | 15.93 | 9.86 | 9.61 | 12.78 | 5.39 | 5.31 |
| K2O | 2.58 | 6.49 | 6.24 | 3.61 | 6.14 | 5.99 | 5.58 | 8.92 | 8.78 |
| P2O5 | 0.02 | 0.05 | 0.05 | 0.03 | 0.05 | 0.05 | 0.71 | 1.13 | 1.12 |
| S2 | 0.04 | 0.10 | 0.10 | 0.00 | 0.00 | 0.00 | 0.51 | 0.81 | 0.80 |
| Cl2 | 4.73 | 0.00 | 0.00 | 2.90 | 0.00 | 0.00 | 2.69 | 0.00 | 0.00 |
| H2O | n.d. | 0.00 | 3.73* | 1.52 | 0.00 | 2.52 | 0.94 | 0.00 | 1.48 |
| LOI | 1.54 | --- | --- | --- | --- | --- | --- | --- | --- |
| Total | 101.88 | 100.00 | 100.00 | 100.57 | 100.00 | 100.00 | 100.90 | 100.00 | 100.00 |
| -O=Cl | 1.07 | | | 0.65 | | | 0.61 | | |
| Total | 100.81 | | | 99.92 | | | 100.29 | | |

* based on LOI value

Table 8. Viscosity estimates with varying water contents following Shaw (1972). Data in log₁₀(poise).

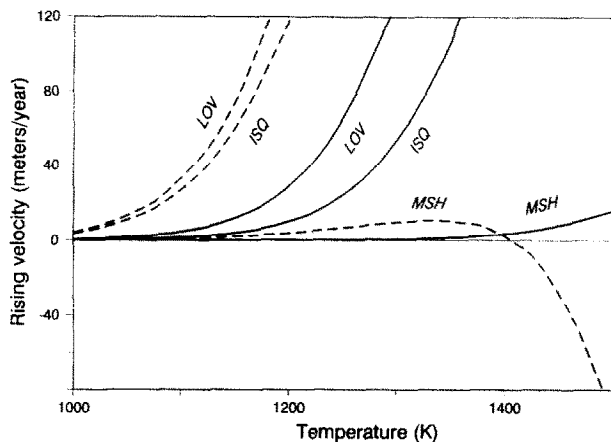| T (K) | MSH | | Ilimaussaq | | Lovozero | |
|---|---|---|---|---|---|---|
| | water content (wt. %) | | | | | |
| | 0.0 | 4.26 | 0.0 | 2.52 | 0.0 | 1.48 |
| 1000 | 10.51 | 6.51 | 7.06 | 5.39 | 8.66 | 7.47 |
| 1200 | 7.91 | 4.69 | 5.13 | 3.79 | 6.41 | 5.46 |
| 1400 | 6.05 | 3.39 | 3.75 | 2.64 | 4.81 | 4.02 |
| 1600 | 4.65 | 2.41 | 2.72 | 1.79 | 3.61 | 2.95 |

FIG. 3. Rising velocities of sodalite phenocrysts (3 mm grain radius) in coexisting melt calculated from Stokes law. Density data from Table 7; viscosity data from Table 8. Solid lines = anhydrous melt, dashed lines = wet melt. ISQ = Ilímaussaq, LOV = Lovozero, MSH = Mont St-Hilaire.

position coexisting with the sodalite phenocrysts is assumed to be the same as the groundmass bulk composition. The groundmass composition was estimated by subtracting the appropriate sodalite components in proportion to the total amount of chlorine in the analysis. The water content of the magma was bracketed between 0 wt% and the water content from the chemical analysis after the removal of the sodalite component. Melt densities are calculated from the models of BOTTINGA *et al.* (1982) and LANGE and CARMICHAEL (1987). The partial molar volume data for $H_2O$ are from the model of BURNHAM and DAVIS (1971) for the albite-water system assuming 3 wt% water in the melt. Magma viscosities are determined from the viscosity data of SHAW (1972).

Whole-rock and calculated groundmass compositions for Mont St-Hilaire, Ilímaussaq and Lovozero are presented in Table 6. The extremely high Cl content of the Mont St-Hilaire analysis leads to a quartz normative calculated groundmass composition. This high chlorine content of the Mont St Hilaire whole rock sample and the purified sodalite was checked by standard wet chemical methods. Samples were finely ground, heated to 500°C for 10 minutes to decrepitate any fluid inclusions and washed in deionized water. Repetitive analyses yield 7.62 ± 0.18 and 4.64 ± 0.10 wt% Cl for the sodalite and whole rock, respectively. The measured chlorine content for the sodalite is 0.3 wt% above the 7.3 wt% maximum for a stoichiometric sample. If 0.3 wt% Cl is subtracted from both the sodalite and the whole-rock sample, then a stoichiometric sodalite and a nepheline normative groundmass composition result. All further calculations were made assuming 4.3 wt% chlorine for the groundmass composition of the Mont St-Hilaire sample. Calculated maximum water contents of 1.5–3.4 wt% $H_2O$ from Mont St-Hilaire, Ilímaussaq and Lovozero are in agreement with estimates of KOSTER VAN GROOS and WYLLIE (1969) and CARMICHAEL *et al.* (1974) for maximum water contents of similar magma chemistries.

Sodalite and melt densities from 1000 to 1600 K are presented in Table 7 for varying water contents. Viscosity estimates for these melts over the same temperature range are

presented in Table 8. Above 1200 K, buoyancy velocities calculated from Stokes law are, in nearly all cases, rapid enough to allow significant reverse cumulation to occur over a period of approximately 1000 years (Fig. 3).

Although sodalite-bearing syenites are rare, their unique chemistry illustrates different properties that occur in igneous processes. The driving force for sodalite buoyancy highlights the importance of crystal settling (and flotation) in large magma chambers and its importance in magma genesis of alkaline rocks.

*Editorial handling:* B. J. Wood

## REFERENCES

AUTEFAGE F. (1980) Variations de la teneur en sodium et en potassium dans des minéraux au cours de leur analyse à la microsonde électronique. *Bull. Minéral.* **103**, 48–53.

BARKER D. S. (1976) Phase relations in the system $NaAlSiO_4$-$SiO_2$-NaCl-$H_2O$ at 400°–800°C and 1 kilobar, and petrologic implications. *J. Geol.* **84**, 97–106.

BEAGLEY B., HENDERSON C. M. B. and TAYLOR D. (1982) The crystal structures of aluminosilicate-sodalites: X-ray diffraction studies and computer modeling. *Mineral. Mag.* **46**, 459–464.

BINSTED N. (1981a) The system Ab-Ne-NaCl-$H_2O$. *Prog. Exp. Petrol., N.E.R.C. Rept.* **5**, 34–36.

BINSTED N. (1981b) The stability of sodalite minerals. *Prog. Exp. Petrol., N.E.R.C. Rept.* **5**, 54–56.

BIRCH F. (1966) Compressibility: elastic constants. In *Handbook of Physical Constants* (ed. S. P. CLARK, JR.); *Geol. Soc. Amer. Mem.* **97**, pp. 97–174.

BOETTCHER A. L. and WYLLIE P. J. (1968) Jadeite stability measured in the presence of silicate liquids in the system $NaAlSiO_4$-$SiO_2$-$H_2O$. *Geochim. Cosmochim. Acta* **32**, 999–1012.

BOHLEN S. R. (1984) Equilibria for precise pressure calibration and a frictionless furnace assembly for the piston-cylinder apparatus. *N. Jb. Mineral. Mh.* **1984**, 404–412.

BOTTINGA Y. and WEILL D. (1970) Densities of liquid silicate systems calculated from partial molar volumes of oxide components. *Amer. J. Sci.* **269**, 169–182.

BOTTINGA Y., WEILL D. and RICHET P. (1982) Density calculations for silicate liquids. I. Revised methods for aluminosilicate compositions. *Geochim. Cosmochim. Acta* **46**, 909–919.

BOWEN N. L. (1912) The binary system: $Na_2Al_2Si_2O_8$ (nephelite, carnegieite)-$CaAl_2Si_2O_6$ (anorthite). *Amer. J. Sci.* **33**, 551–573.

BOWEN N. L. and GREIG N. L. (1925) The crystalline modifications of $NaAlSiO_4$. *Amer. J. Sci.* **10**, 204–215.

BROUSSE R., VARET J. and BIZOUARD H. (1969) Iron in the minerals of the sodalite group. *Contrib. Mineral. Petrol.* **22**, 169–184.

BURNHAM C. W. and DAVIS N. F. (1971) The role of $H_2O$ in silicate melts I. *P-V-T* relations in the system $NaAlSi_3O_8$-$H_2O$ to 10 kilobars and 1000°C. *Amer. J. Sci.* **270**, 54–79.

CAMPBELL I. H., ROEDER P. L. and DIXON J. M. (1978) Plagioclase buoyancy in basaltic liquids as determined with the centrifuge furnace. *Contrib. Mineral. Petrol.* **67**, 369–377.

CARMICHAEL I. S. E., TURNER F. J. and VERHOOGEN J. (1974) *Igneous Petrology.* McGraw-Hill, 739p.

CHASE M. W., JR., DAVIES C. A., DOWNEY J. R., JR., FRURIP D. J., MCDONALD R. A. and SYVERUD A. N. (1985) *JANAF Thermochemical Tables,* 3rd edn., Vol. 14, Amer. Chem. Soc., Midland, MI. 926p.

CLARK S. P. (1959) Effect of pressure on the melting points of eight alkali halides. *J. Chem. Phys.* **31**, 1526–1531.

COHEN L. H. and KLEMENT W., JR. (1976) Effect of pressure on reversible solid-solid transitions in nepheline and carnegieite. *Mineral. Mag.* **40**, 487–492.

CURRIE K. L., EBY G. L. and GITTINS J. (1986) The petrology of the Mont Saint Hilaire complex, southern Quebec: An alkaline gabbro-peralkaline syenite association. *Lithos* **19**, 65–81.

DEER W. A., HOWIE R. A. and ZUSSMAN J. (1963) *Rock-Forming Minerals*, Vol. 4. Wiley. 435p.

DEMIDENKO V. A., ASTAKHOVA V. V. and VOLYNETS F. K. (1983) The structural transitions of sodalite. *Kristallografiya* **28**, 593–595.

DONNAY G., SCHAIRER J. F. and DONNAY J. D. H. (1959) Nepheline solid solutions. *Mineral. Mag.* **32**, 93–109.

FYFE W. S., TURNER F. J. and VERHOOGEN J. (1958) Metamorphic reactions and metamorphic facies. *Geol. Soc. Amer. Mem.* **73**, 259p.

GOLDSMITH J. R. and JENKINS D. M. (1984) The high-low albite relations revealed by reversal of degree of order at high pressures. *Amer. Mineral.* **70**, 911–923.

GROSSMAN L. and STEELE I. M. (1976) Amoeboid olivine aggregates in the Allende meteorite. *Geochim. Cosmochim. Acta* **40**, 149–155.

HAMILTON E. I. (1964) The geochemistry of the northern part of the Ilímaussaq intrusion, S. W. Greenland. *Medd. Grønland* **162**, 1–104.

HASSAN I. and GRUNDY H. D. (1984) The crystal structures of so-dalite-group minerals. *Acta Cryst.* **B40**, 6–13.

HAYS J. F. and BELL P. M. (1973) Albite-jadeite-quartz equilibrium: A hydrostatic determination. *Carnegie Inst. Wash. Yb.* **72**, 706–708.

HAZEN R. M. and SHARP Z. D. (1988) Compressibility of the framework silicates sodalite and scapolite. *Amer. Mineral.* **73**, 1120–1122.

HELFFRICH G. R., SHARP Z. D. and ESSENE E. J. (1986) Thermodynamics of sodalite and implications of sodalite presence in syenitic systems. *Eos* **67**, 389.

HELGESON H. C., DELANY J. M., NESBITT H. W. and BIRD D. K. (1978) Summary and critique of the thermodynamic properties of rock-forming minerals. *Amer. J. Sci.* **278a**, 1–229.

HENDERSON C. M. B. and ROUX J. (1976) The thermal expansions and crystallographic transformations of some synthetic nephelines. *Prog. Exp. Petrol., N.E.R.C. Rept.* **3**, 60–69.

HENDERSON C. M. B. and ROUX J. (1977) Inversions in sub-potassic nephelines. *Contrib. Mineral. Petrol.* **61**, 279–298.

HENDERSON C. M. B. and TAYLOR D. (1978) The thermal expansion of synthetic aluminosilicate-sodalites, $M_8(Al_6Si_6O_{24})X_2$. *Phys. Chem. Mineral.* **2**, 337–347.

HENDERSON C. M. B. and TAYLOR D. (1979). Infrared spectra of aluminogermanate- and aluminate-sodalites, and a re-examination of the relationship between *T-O* bond length, *T-O-T* angle and the position of the main *IR* absorption band for compounds with framework structures. *Spectrochim. Acta* **A:35**, 925–935.

HENDERSON C. M. B. and THOMPSON A. B. (1980) The low-temperature inversion in sub-potassic nephelines. *Amer. Mineral.* **65**, 970–980.

HUMMEL F. A. (1949) Properties of some substances isostructural with silica. *J. Amer. Ceram. Soc.* **32**, 320–326.

IRVINE T. N. (1987) Layering and related structures in the Duke Island and Skaergaard intrusions: similarities, differences, and origins. In *Origins of Igneous Layering* (ed. I. PARSONS), pp. 185–245. D. Reidel Publishing.

JANZ G. J. (1967) *Molten Salts Handbook.* Academic Press, 588p.

JOHANNES W. (1978) Pressure comparing experiments with NaCl, AgCl, talc, pyrophyllite assemblies in a piston-cylinder apparatus. *N. Jb. Mineral. Mh.* **1978(2)**, 84–92.

KELLEY K. K., TODD S. S., ORR R. L., KING E. G. and BONNICKSON K. R. (1953) Thermodynamic properties of sodium-aluminum and potassium-aluminum silicates. *U.S. Bur. Mines Rept.* **4955**, 21p.

KILINC I. A. and BURNHAM C. W. (1972) Partitioning of chloride between a silicate melt and coexisting aqueous phase from 2 to 8 kilobars. *Econ. Geol.* **67**, 231–235.

KLINGENBERG R. and FELSCHER J. (1981) Crystal data for the low-

temperature form of carnegieite NaAlSiO₄. *J. Appl. Cryst.* **14**, 66–68.

KLINOWSKI J., CARR S. W., TARLING S. E. and BARNES P. (1987) Magic-angle-spinning NMR shows the aluminosilicate framework of ultramarine to be disordered. *Nature* **330**, 56–58.

KOMADA N., WESTRUM E. F., JR., HEMINGWAY B. S., ZOLOTOV M. Y., SEMENOV Y. V., KHODAKOVSKY I. L. and ANOVITZ L. M. (1989) Thermodynamic properties of sodalite from 15 to 1000 K. *J. Chem. Therm.* (in prep.).

KOSTER VAN GROOS A. F. and WYLLIE P. J. (1969) Melting relationships in the system $NaAlSi_3O_8$-NaCl-$H_2O$ at one kilobar pressure, with petrological applications. *J. Geol.* **77**, 581–605.

LANGE R. A. and CARMICHAEL I. S. E. (1987) Densities of $Na_2O$-$K_2O$-CaO-MgO-FeO-$Fe_2O_3$-$Al_2O_3$-$TiO_2$-$SiO_2$ liquids: New measurements and derived partial molar properties. *Geochim. Cosmochim. Acta* **51**, 2931–2946.

LIU L. (1977) High pressure $NaAlSiO_4$: The first silicate calcium ferrite isotype. *Geophys. Res. Lett.* **4**, 183–186.

LOEWENSTEIN W. (1954) The distribution of aluminum in the tetrahedra of silicates and aluminates. *Amer. Mineral.* **39**, 92–96.

LONS J. and SCHULZ H. (1967) Strukturverfeinerung von Sodalith, $Na_8Si_6Al_6O_{24}Cl_2$. *Acta Cryst.* **23**, 434–436.

LUMPKIN G. R. (1980) Nepheline and sodalite in a barred olivine chondrule from the Allende meteorite. *Meteoritics* **15**, 139–147.

McCONNELL J. D. C. (1981) Time-temperature study of the intensity of satellite reflections in nepheline. *Amer. Mineral.* **66**, 990–996.

MIRWALD P. W., GETTING I. C. and KENNEDY G. C. (1975) Low-friction cell for piston-cylinder high-temperature apparatus. *J. Geophys. Res.* **80**, 1519–1525.

NEWTON M. S. and KENNEDY G. C. (1968) Jadeite, analcite, nepheline, and albite at high temperatures and pressures. *Amer. J. Sci.* **266**, 728–735.

PETERSON R. C. (1983) The structure of hackmanite, a variety of sodalite from Mont St-Hilaire, Quebec. *Can. Mineral.* **21**, 549–552.

PIOTROWSKI J. M. and EDGAR A. D. (1970) Melting relations of undersaturated alkaline rocks from South Greenland, *Medd. Grønland* **181**, 1–62.

ROBIE R. A., HEMINGWAY B. S. and FISHER J. R. (1978) Thermodynamic properties of minerals and related substances at 298.15 K and 1 bar ($10^5$ pascals) pressure and at higher temperatures. *U.S. Geol. Surv. Bull.* **1452**, 456p. (reprinted with corrections).

ROBINSON G. R., JR. and HAAS J. L., JR. (1983) Heat capacity, relative enthalpy, and calorimetric entropy of silicate minerals: an empirical method of prediction. *Amer. Mineral.* **68**, 541–553.

ROBINSON G. R., JR., HAAS J. L., JR., SCHAFER C. M. and HASELTON H. T., JR. (1982) Thermodynamic and thermophysical properties of selected phases in the $MgO$-$SiO_2$-$H_2O$-$CO_2$, CaO-$Al_2O_3$-$SiO_2$-$H_2O$-$CO_2$, and Fe-FeO-$Fe_2O_3$-$SiO_2$ chemical systems, with special emphasis on the properties of basalts and their mineral components. *U.S. Geol. Surv. Open-File Rept. 83–79*, 429p.

ROEDDER E. (1984) *Fluid Inclusions; Reviews in Mineralogy 12.* Mineral. Soc. Amer., 644p.

ROY D. M. and ROY R. (1969) The carnegieite-nepheline and cristobalite-tridymite transition. *Ind. Mineral.* **10**, 16–22.

SEMENOV Y. V., SIDOROV Y. I., KHODAKOVSKII I. L., ZHDANOV V. M. and TURDAKIM V. A. (1981) Standard entropy of minerals. *Vses. Soveshch. Eksp. Tekh. Mineral. Petrogr., (Mater.), 10th.* (ed. Y. P. MEL'NIK and D. NAUKOVA), pp. 96–102. Kiev, U.S.S.R.

SHANNON R. D. and BERZINS T. (1979) Ionic conductivity in low carnegieite compositions based on $NaAlSiO_4$. *Mat. Res. Bull.* **14**, 361–367.

SHAW H. R. (1972) Viscosities of magmatic silicate liquids: an empirical method of prediction. *Amer. J. Sci.* **272**, 870–893.

SIMPSON E. S. W. and OTTO J. D. T. (1960) On the Pre-Cambrian anorthosite mass of southern Angola. *Rept. 21st Intern. Geol. Congr., Norden* **13**, 216–227.

SKINNER B. J. (1966) Thermal expansion. In *Handbook of Physical Constants.* (ed. S. P. CLARK, JR.); *Geol. Soc. Amer. Mem. 97*, pp. 75–96.

SMITH J. V. and TUTTLE O. F. (1957) The nepheline-kalsilite system: I. X-ray data for the crystalline phases. *Amer. J. Sci.* **255**, 282–305.

SOBOLEV V. S., BAZAROVA T. Y., SHUGUROVA N. A., BAZAROV L. SH., DOLGOV YU. A. and SÖRENSEN H. (1970) A preliminary examination of fluid inclusions in nepheline, sorensenite, tugtupite and chkalovite from the Ilímaussaq alkaline intrusion, South Greenland. *Medd. Grønland* **181,** 1–32.

SÖRENSEN H. (1958) The Ilímaussaq batholith, a review and discussion. *Medd. Grønland* **162,** 1–48.

STOPLER E., WALKER D., HAGER B. H. and HAYS J. F. (1981) Melt segregation from partially molten source regions: the importance of melt density and source region size. *J. Geophys. Res.* **86,** 6261–6271.

STORMER J. C. and CARMICHAEL I. S. E. (1971) The free energy of sodalite and the behavior of chloride, fluoride and sulfate in silicate melts. *Amer. Mineral.* **56,** 292–306.

THOMPSON A. B. and PERKINS E. H. (1981) Lambda transitions in minerals. In *Thermodynamics of Minerals and Melts* (ed. R. C. NEWTON, A. NAVROTSKY and B. J. WOOD); *Adv. in Phys. Geochem. 1,* pp. 35–62.

TOMISAKA T. and EUGSTER H. P. (1968) Synthesis of the sodalite group and subsolidus equilibria in the sodalite-noselite system. *Mineral. J.* **5,** 249–275.

TUTTLE O. F. and SMITH J. V. (1958) The nepheline-kalsilite system: II. Phase relations. *Amer. J. Sci.* **256,** 571–589.

USSING N. V. (1912) Geology of the country around Julianehaab, Greenland. *Medd. Grønland* **38,** 1–376.

VLASOV K. A., KUZ'MENKO M. Z. and ES'KOVA E. M. (1966) *The Lovozero Alkali Massif.* Hafner Publishing, 627p.

WELLMAN T. R. (1969a) The stability of sodalite in the system NaAlSi₃O₈-KAlSi₃O₈-NaAlSiO₄-KAlSiO₄-NaCl-KCl-H₂O. Ph.D. dissertation, Yale Univ.

WELLMAN T. R. (1969b) The vapor pressure of NaCl over decomposing sodalite. *Geochim. Cosmochim. Acta* **33,** 1302–1303.

WELLMAN T. R. (1970a) The stability of sodalite in a synthetic syenite plus aqueous chloride fluid system. *J. Petrol.* **11,** 49–71.

WELLMAN T. R. (1970b) Fugacities and activity coefficients of NaCl in NaCl-H₂O fluids at elevated temperatures and pressures. *Amer. J. Sci.* **269,** 402–413.

WESTRUM E. F., JR. (1974) Calorimetry of phase and ordering transitions. *Pure Appl. Chem.* **38,** 539–555.

WOOD B. J. and FRASER D. G. (1977) *Elementary Thermodynamics for Geologists.* Oxford Univ. Press, 303p.

ZOLOTOV M. Y., SEMENOV Y. V., SIDOROV Y. I., ZHDANOV V. M. and TURDAKIM V. A. (1982) Thermodynamic properties of sodalite. In *Papers of All-Union Conference. Problems of Calorimetry and Chemical Thermodynamics,* Vol. 2, pp. 451–453. Chernogolovka.